J Solid State Electrochem (2008) 12:155–163
DOI 10.1007/s10008-007-0375-4

ORIGINAL PAPER

The inhibiting effect of cobalt(III)–*cyclam* complexes with substituted β-diketones on iron corrosion in perchlorate solution

Ksenija Babić-Samardžija · Norman Hackerman · Sofija P. Sovilj · Vladislava M. Jovanović

Received: 4 April 2007 / Revised: 10 May 2007 / Accepted: 7 June 2007 / Published online: 8 August 2007

Abstract The inhibiting effect of cobalt(III) complexes with macrocyclic ligand *cyclam* (1,4,8,11-tetraazacyclotetradecane) and β-diketonato ligands have been investigated on iron corrosion in 0.1 M $HClO_4$ by potentiodynamic, linear polarization resistance (LPR), and electrochemical impedance spectroscopy (EIS) measurements. Analysis of the polarization curves and impedance spectra, by adding complex compounds to the acid solution and comparing with inhibitor-free solution, show corrosion current decrease and charge transfer resistance increase, respectively. Impedance data are fitted with equivalent circuit models. The stability of the adsorbed film was followed by LPR. Scanning electron microscopy (SEM) was used to screen physical changes of the reacted surfaces both treated and untreated. The differences in inhibitor efficiencies depend on the substituent group of the coordinated β-diketone ligand. Structural and electronic properties of this group of compounds in relation to inhibitor efficiency were analyzed by using the molecular modeling structures and correlated with previously reported spectroscopy data.

Keywords Iron electrode · Perchloric acid · Corrosion inhibition · Co(III) complexes

K. Babić-Samardžija · N. Hackerman
Chemistry Department MS60, Rice University,
Houston, TX 77005, USA

S. P. Sovilj
Faculty of Chemistry, University of Belgrade,
P.O. Box 158, 11000 Belgrade, Serbia

V. M. Jovanović
ICTM, Department of Electrochemistry,
P.O. Box 473 11000, Belgrade, Serbia

Present address:
K. Babić-Samardžija (✉)
Baker Petrolite Corp.,
12645 W. Airport Blvd.,
Sugar Land, TX 77478, USA
e-mail: kbabic@rice.edu

Introduction

Most corrosion inhibitors are nitrogen-, sulfur-, or oxygen-containing organic compounds. They inhibit dissolution of metals in aggressive environments by adsorption and/or bridging with other solution components to form a protecting layer. The attachment is often largely a function of their molecular structure [1].

It has been shown that mixed-ligand Co(III) complexes with macrocyclic polyamine could be a new class of corrosion inhibitors of iron in acidic solution [2, 3]. An important factor in the formation of mixed-ligand complexes is to minimize steric hindrance. This can be accomplished by a suitable combination of bulky and slim ligands, like macrocyclic polyamine 1,4,8,11-tetraazacyclotetradecane (*cyclam*) and diketone, respectively. Beside four *trans*- configurations, 14-membered macrocyclic ring could be folded in *cis*- configuration in the presence of some bidentate ligands [4–10].

β-Dicarbonyl compounds present a class of important and widely investigated organic molecules [11, 12]. They exhibit a variety of coordination modes [12]. The chelating structure of β-diketone ligands has been investigated in various transition metal complexes [13–15]. Specific molecule stabilization is realized by intramolecular hydrogen bonds in the structure of the enol "pseudoaromatic" ring, which make possible formation of metal ion-ligand π-bond [12]. Acetylacetone (*acac*), perhaps the best known

β-diketone and derived β-diketones with different R-groups (*Rac*), have been studied extensively not only in terms of their ability to complex many metal ions [11–17] but also in their application in biomedicine [18], in production of homogeneous and heterogeneous catalysts [19, 20], petroleum industry as fuel additives [21], vapor-plating of metals [22], and manufacturing of superconducting thin films [23].

Thus, complexes with the MN_4 chromophore are interesting not only from structural aspect but also appear to be a promising class of materials [24]. Both structural and electronic factors may simultaneously affect their spectral as well as electrochemical characteristics such as the reduction of oxygen [25–27], electrochemical redox peak potentials [5, 27], and catalytic features [5] of the complexes. For example, cyclic voltammograms (CV) of these complexes in aqueous solution show a reverse redox Co^{III}/Co^{II} peak in the cathodic region and some influence on the cathodic hydrogen evolution reaction [27]. Both processes are influenced by the presence of different β-diketone ligands. The absence of any peaks in nonaqueous solution indicates stabilization of both macrocyclic and chelate ligand through the coordination to cobalt(III). Furthermore, the results obtained at glassy carbon (GC) rotating electrode in O_2-saturated perchlorate solution show oxygen reduction in the presence of these complexes, shifting the potential anodically and increasing the current [27].

The aim of this work was to study possible application of this type of compounds as corrosion inhibitors. Four macrocyclic cobalt(III)–*cyclam* complexes with β-diketones, i.e., 2,4-pentanedionato (*acac*), 1,3-diphenyl-1,3-propanedionato (*dibzac*), 1,1,1,5,5,5-hexafluoro-2,4-pentanedionato (*hfac*), or 2,2,6,6-tetramethyl-3,5-heptanedionato (*tmhd*) ions, were investigated electrochemically for corrosion inhibition of iron in 0.1 M $HClO_4$. Their inhibitor properties were followed by using the potentiodynamic and linear polarization resistance (LPR), and electrochemical impedance spectroscopy (EIS) measurements. Scanning electron microscopy (SEM) was used to monitor morphological changes of the reacted surfaces. Some calculated structural and electronic properties of complex compounds in relation to their inhibitor efficiencies were analyzed and correlated with previously reported spectroscopy data.

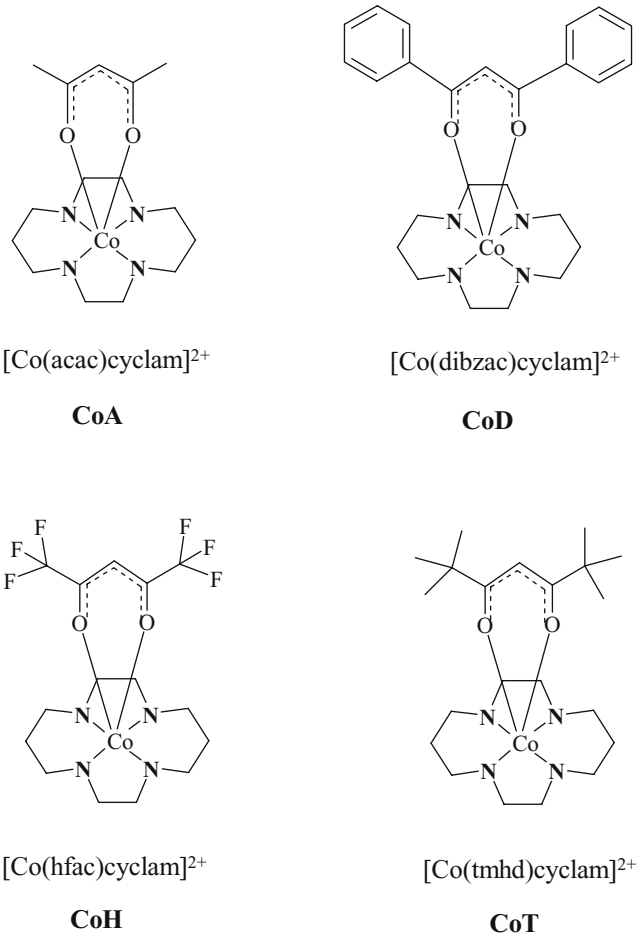

Fig. 1 The structure of complexes of the general formula [Co(Rac)cyclam]$^{2+}$

Experimental

Materials

The chemical structures of the cobalt(III) complexes studied are presented in Fig. 1 along with the acronyms used throughout the text. All of the compounds were obtained by direct synthesis from $Co(ClO_4)_2 \cdot 6H_2O$, *cyclam* and β-diketone (Aldrich Chemical) as described in literature [7, 8]. They were added to the 0.1 M $HClO_4$ (Fisher Scientific) at 10^{-5} to 10^{-3} M concentration range.

Experiments were carried out using pure iron (Puratronic 99.99%, Johnson Matthey) as the working electrode. The iron rod, 5 mm in diameter was mounted in Teflon. Exposed surface was abraded with emery papers of decreasing grit size (180, 120, 0, and 4/0), polished with 0.5 μm Al_2O_3, cleaned ultrasonically in 18 MΩ water, and rinsed in acetone and bidistilled water. The iron electrode was immersed in acid or in inhibitor-containing solutions 1 h before starting the measurements.

Methods

A conventional electrochemical cell was used in the experiments. The counter electrode was platinum (Premion® 99.997% with 99.9% Pt gauze-52 mesh, Johnson Matthey) and the reference electrode was saturated calomel (SCE). Reported potentials were measured vs SCE. The experiments were carried out under static conditions at 25 °C in

aerated solutions. A Luggin fine capillary was placed close to the working electrode to minimize ohmic resistance.

Measurements were performed using a Gamry Instrument Potentiostat/Galvanostat/ZRA. This includes a Gamry Framework system based on the ESA400 and the VFP600, and Gamry applications that include DC105 corrosion and EIS300, along with a computer for collecting the data. Echem Analyst 4.0 Software was used for plotting, graphing, and fitting data. The current–potential curves were obtained by changing the electrode potential automatically from −250 mV_{SCE} to +250 mV_{SCE} at a scan rate of 1 mV s^{-1}. LPR experiments were done at −25 mV to +25 mV vs open circuit potential (E_{oc}) at a scan rate of 0.125 mV s^{-1}. EIS measurements were carried out over the frequency range of 100 kHz to 0.1 Hz with amplitude of 5 mV peak-to-peak using *ac* signals at E_{oc}.

The physical changes of the reacted surfaces were obtained by using a FEI XL-30 environmental scanning electron microscope (ESEM). The samples for SEM measurements prepared by the same procedure as for the electrochemical experiments with iron foil (99.99%, 0.25 mm thick, Johnson Matthey) being used as the working electrode instead of the iron rod. Polished foil surface (approximately 1 cm^2) was cleaned ultrasonically in 18 MΩ water, rinsed in acetone and bidistilled water and immersed in acid or in inhibitor-containing solutions for 1 h. The samples were dried under vacuum before placing in the SEM vacuum chamber. The images were taken using a beam of 30 kV in range of 1000–6500 magnitude. During the measurements, the main chamber pressure was ~1.5×10^{-5} mBar.

Hyperchem Version 7 (Hypercube), a quantum-mechanical program for molecular modeling was used for molecular orbital calculations. These are based on the semiempirical self-consistent field molecular orbital (SCF-MO) theory. A full optimization of all geometric variables without any symmetry constraints was performed at the restricted Hartree-Fock (RHF) level. For these calculations, the approach of ZINDO/1 method optimized especially for computing properties of transition elements' compounds was used as the most appropriate for energy and structure determination. ZINDO/1 is based on the intermediate neglect of differential overlap (INDO) approximation [28].

Results and discussion

Electrochemical DC and AC measurements

Corrosion protection of iron in perchlorate solution by cobalt(III)–*cyclam* complexes with substituted β-diketones was studied by potentiodynamic and linear polarization measurements as well as by electrochemical impedance spectroscopy. Electrochemical parameters of iron corrosion in the presence of these complexes are summarized in Table 1. Corrosion current (i_{corr}), corrosion potential (E_{corr}) as well as anodic and cathodic slopes (β_a and β_c) were derived from the extrapolation of the *E*/*I* curves. Inhibitor efficiency (IE) was calculated taking in account i_{corr} as in Eq. (1). Here, i^o_{corr} and i_{corr} are uninhibited and inhibited corrosion current densities, respectively.

$$IE = \left(\frac{i^o_{corr} - i_{corr}}{i^o_{corr}}\right) \times 100 \quad (1)$$

According to the DC method, cobalt complexes show anticorrosion properties in the investigated concentration

Table 1 Electrochemical corrosion parameters of iron in 0.1 M $HClO_4$ in the presence of different concentrations of Co(III) complexes, derived from potentiodynamic polarization measurements

Compound	Conc. (M)	i_{corr} (μA cm^{-2})	$-E_{corr}$ (mV)	β_a (mV dec^{-1})	β_c (mV dec^{-1})	IE (%)
Blank	–	216.0	520.8	108.1	277.8	–
CoT	10^{-5}	32.2	508.1	45.5	262.1	85.1
	10^{-4}	23.5	524.4	39.8	253.2	89.1
	5×10^{-4}	21.3	528.8	53.2	252.9	90.1
	10^{-3}	14.5	525.5	42.2	243.0	93.3
CoD	10^{-5}	34.7	532.4	52.8	282.6	83.9
	10^{-4}	25.5	536.0	57.1	281.8	88.2
	5×10^{-4}	22.2	529.4	50.2	267.1	89.7
	10^{-3}	15.4	543.6	42.5	265.2	92.8
CoH	10^{-5}	37.3	532.4	56.8	312.2	82.7
	10^{-4}	29.0	540.5	60.5	269.2	86.6
	5×10^{-4}	22.6	535.0	51.6	263.7	89.5
	10^{-3}	15.5	537.3	43.6	224.4	92.8
CoA	10^{-5}	37.4	520.7	56.2	323.5	82.6
	10^{-4}	35.7	525.3	56.7	284.7	83.5
	5×10^{-4}	26.4	524.5	51.8	268.0	87.7
	10^{-3}	19. 8	525.3	44.9	251.3	90.8

range (Table 1 and Fig. 2). Compared with an inhibitor-free solution where i_{corr} reaches 216 μA cm^{-2}, these inhibitors decrease corrosion current to 14–37 μA cm^{-2}. Generally, i_{corr} decreases with increasing inhibitor concentration. The IE increases considerably with inhibitor concentration, up to 93%. Even at 10^{-5} M, the inhibiting effect is fair to good. The lowest effectiveness comes with CoA while the other cobalt(III)–*cyclam* complexes show a similar range of efficiency in the order of CoT > CoD > CoH.

The profile of the Tafel lines (Fig. 2) illustrates inhibitory effect in presence of these compounds. These inhibitors suppress both anodic and cathodic reaction. Cathodic inhibition intensifies with concentration (Fig. 2a and Table 1). The anodic reaction is slightly influenced at lower concentration (Fig. 2b) but more significantly at 10^{-3} M (Table 1). Stern-Geary "constant" $-B$ value [29] (and βs) suggests that polarization is due to a combination

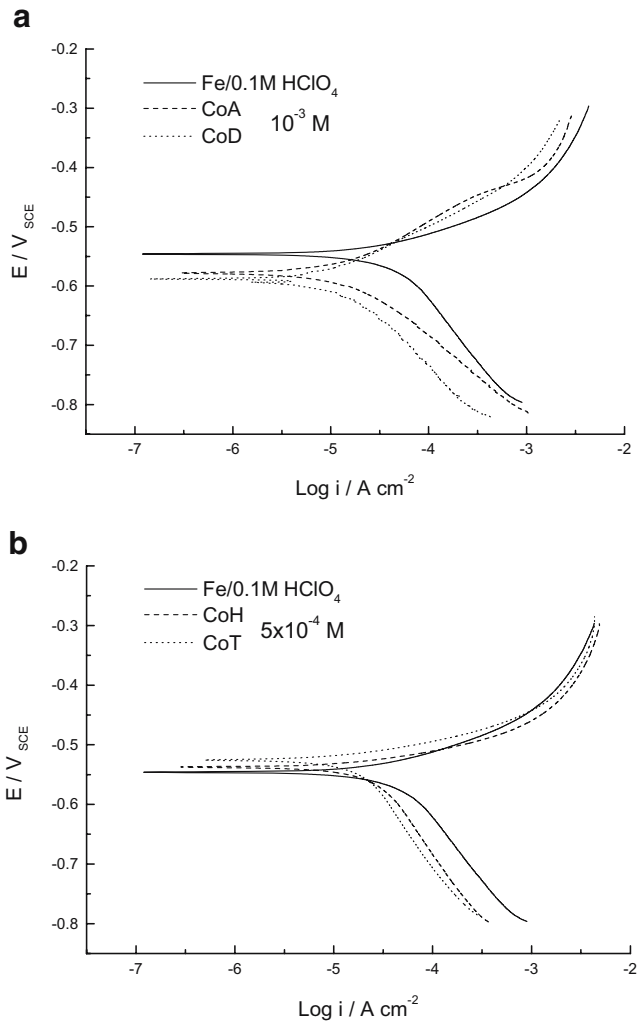

Fig. 2 Anodic and cathodic polarization curves for iron in 0.1 M $HClO_4$ and in the presence of **a** CoA and CoD at 10^{-3} M; **b** CoH and CoT at 5×10^{-4} M

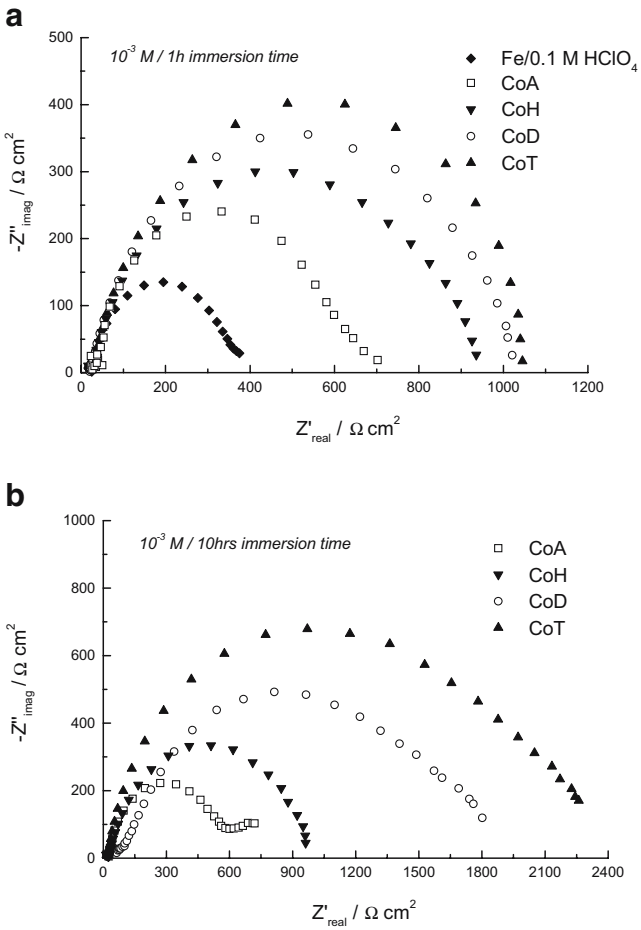

Fig. 3 Nyquist plots for iron in 0.1 M $HClO_4$ and in the presence of 10^{-3} M Co(III) complexes after **a** 1 h of immersion; **b** 10 h of immersion

of activation controlled anodic process and diffusion controlled cathodic process.

Impedance spectra for iron in perchloric acid in the presence of Co(III) complexes were measured under potentiostatic conditions after 1 and 10 h of immersion. A corresponding set of Nyquist plots is given in Fig. 3. Charge transfer resistance (R_{ct}) was evaluated from the Nyquist plots as the difference in impedance at the lower and higher frequencies and is shown for different concentrations of complexes compounds in Fig. 4a. Double layer capacitance (C_{dl}) is calculated from the R_{ct} and the maximum imaginary component of the impedance ($-Z''_{max}$) [3] and is presented in Fig. 4b.

The R_{ct} obtained from the Nyquist plots show that R_{ct} increase in the presence of cobalt complexes (Fig. 3a). After prolonged immersion time (Fig. 3b) resistance is almost doubled for CoT (1,023 vs 2,260 Ωcm^2) and CoD (1,017 vs 1,802 Ωcm^2) but less evident for CoH (936 vs 962 Ωcm^2) and CoA (728 vs 793 Ωcm^2) for 1 vs 10 h immersion, respectively. For CoH and CoA, inhibition effect after longer immersion increases for about 10%.

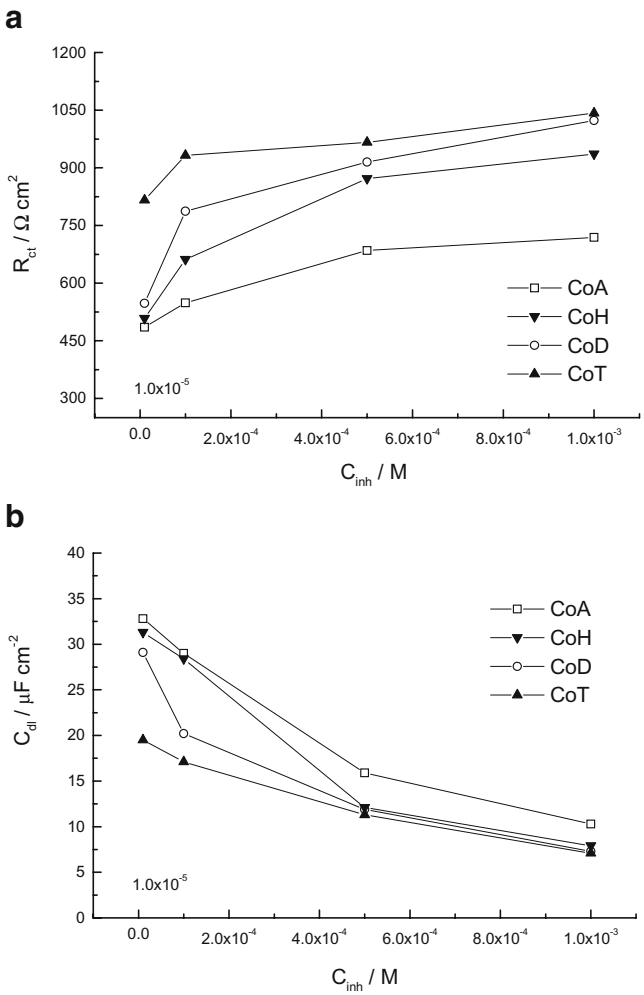

Fig. 4 Correlation between **a** charge transfer resistance; **b** double layer capacitance and inhibitor concentration for the investigated Co (III) complexes in 0.1 M $HClO_4$

Charge transfer resistance increases with inhibitor concentration (Fig. 4a). The presence of CoH, CoD, and CoT in acid demonstrates nearly equal inhibitor properties at 5×10^{-4} M but with CoA there is less inhibition. This suggests that inhibitor treatment has different influence because of substituted β-diketone moiety, i.e., hexafluoro-, diphenyl-, and *tert*-butyl R-groups in CoH, CoD, and CoT complexes, respectively.

Double-layer capacitance (C_{dl}) values tend to decrease by increasing the concentration of cobalt complexes as Fig. 4b indicates. This suggests that these molecules act by adsorption on the metal/solution interface [30]. The value of C_{dl} depends on many variables, e.g., electrode potential, temperature, solution components, oxide layers, surface roughness, etc. Generally, the effect is related to the local dielectric constant decrease and/or an increase in the thickness of the electrical double layer.

EIS spectra were analyzed with an equivalent electrical circuit model. The impedance is affected by the interaction between frequency and all of the physical and chemical processes that respond to that frequency change, within the electrochemical cell and across the corroding interface [31]. Equivalent circuits shown in Fig. 5 represent models to fit the EIS data of the investigated inhibitor molecules. R_1, R_2, and CPE refer to solution and charge transfer resistance, and constant phase element, respectively. The first model, Fig. 5a, corresponds to circuit elements described as semi-circles in EIS spectra. These spectra indicate charge transfer reactions with parallel capacitor and resistor. CPE have been commonly used in the impedance spectra as result of surface heterogeneities and diffusion processes affected by frequency (Warburg impedance, W) [32]. Therefore the semicircle at high frequencies corresponds to the faradic charge-transfer behavior while at low frequencies linear diffusion process describes the "Warburg" impedance (Fig. 5b).

The first equivalent circuit (Fig. 5a) corresponds to the charge transfer reaction of CoH and CoT complexes. Figure 6a and b demonstrates equivalent circuit (EC) fitting data for Nyquist and Bode-phase plots of iron corrosion in 0.1 M $HClO_4$ at E_{corr} in the presence of these compounds in concentration of 10^{-3} M. R_1 and R_2 were calculated from the real axis value at the high frequency intercept and as diameter of semicircle, respectively. The EC in Fig. 5b and fitting plots in Fig. 7 correspond to surface reaction of the compounds CoD and CoA in 10^{-5} and 10^{-4} M solutions, respectively. The impedance depends on the frequency of the potential perturbation. At high frequency the Warburg frequency is small while at low frequencies the reactants diffuse farther [32–34]. In the presence of CoA, the diffusion process appears to be at all concentration studied while with CoD, at 10^{-3} M after 10 h of immersion the impedance spectra correspond to charge transfer reaction as in case of CoH and CoT. In case of finite thickness, impedance will

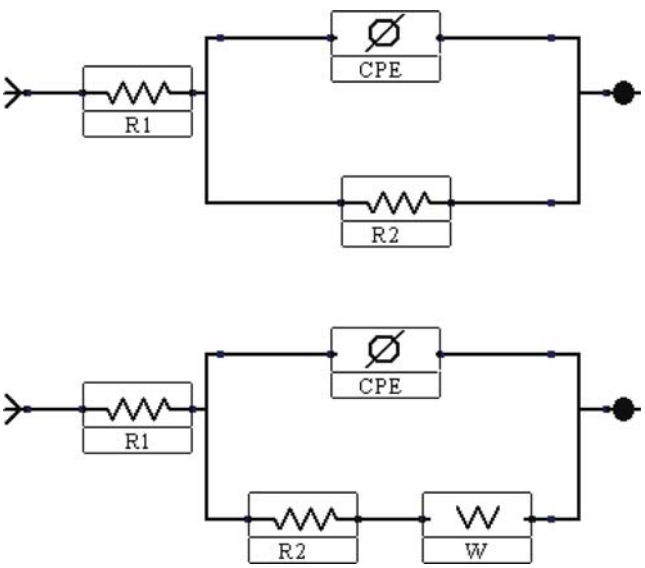

Fig. 5 Equivalent circuit models for the studied inhibitors

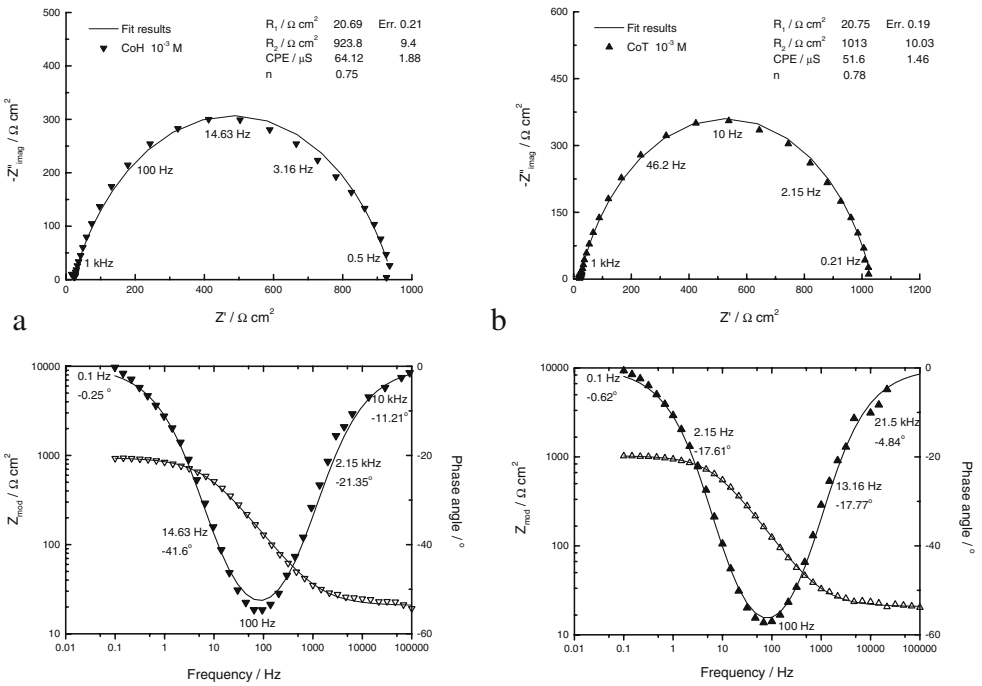

Fig. 6 Nyquist and Bode-phase plots of iron corrosion at E_{corr} in 0.1 M $HClO_4$ in the presence of **a** 10^{-3} M CoH and **b** 10^{-3} M CoT

exhibit charge transfer dominated regime [35]. For CoA, diffusion process in a narrow range of low frequencies is related to very thin film on metal surface [36].

To confirm the stability of the adsorbed inhibitor layer on the surface the set of LPR, experiments were performed after 1 to 10 h of immersion with 10^{-3} M CoD inhibitor-containing solution. Polarization resistance (R_p) increases with immersion time and corrosion current density decreases, as shown in Table 2. Afterward, polarization resistance was measured in perchloric acid to inspect stability of inhibitor film adsorbed on the surface. When immersion time is 1 h, the instantaneous corrosion rate is close to that of the 10^{-3} M CoD inhibitor/acid solution (627 vs 655 Ωcm^2, Table 2). Longer immersion in acid (5 to 10 h) points out that polarization resistance slightly increases. After 10 h of immersion, stability of adsorbed inhibitor film is evident in

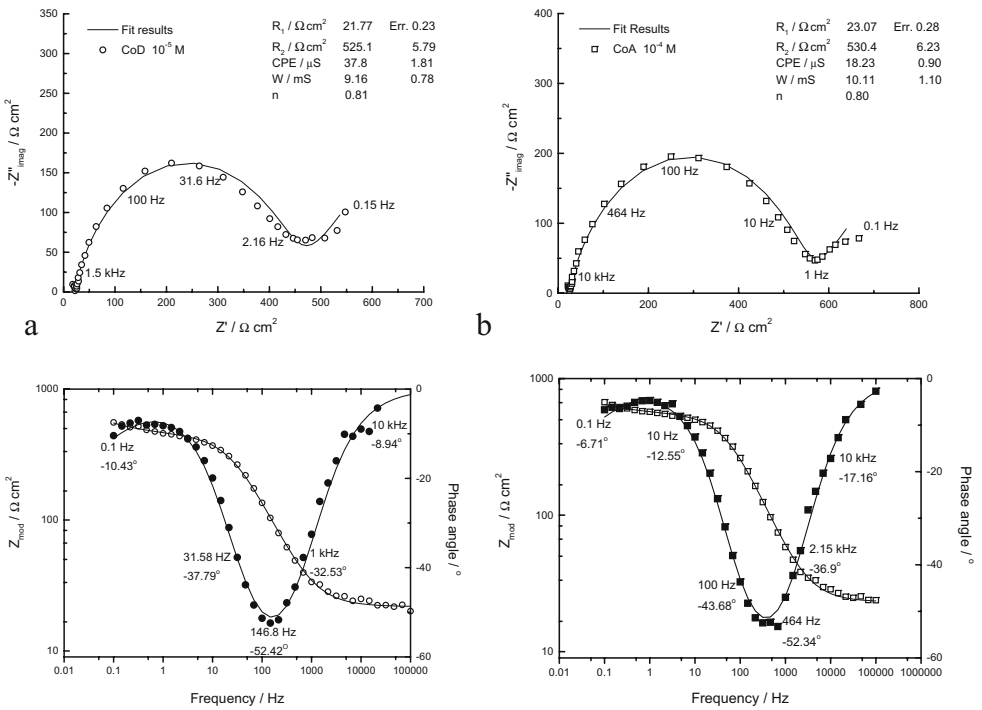

Fig. 7 Nyquist and Bode-phase plots of iron corrosion at E_{corr} in 0.1 M $HClO_4$ in the presence of **a** 10^{-4} M CoA and **b** 10^{-5} M CoD

Table 2 LPR data of iron in 0.1 M $HClO_4$ after 1 to 10 h of immersion in 10^{-3} M CoD solution

Compound	Immersion time (h)		R_p (Ω cm^2)	$-E_{corr}$ (mV)	i_{corr} (μA cm^{-2})
	CoD	Acid			
10^{-3} M CoD in 0.1 M $HClO_4$	1		627	528.3	41.5
	5		1,150	570.8	22.6
	10		1,699	550.6	15.3
	1	0	655	577.0	39.8
		1	700	595.9	37.2
		5	830	600.0	31.4
		10	1,074	588.0	24.3
	10	0	1,055	554.8	24.7
		1	1,198	560.8	21.8
		5	1,535	562.3	17.0
		10	1,557	565.9	16.7

$HClO_4$ acid. This in turn means strong interaction at the electrode/electrolyte interface that preserves iron surface from the acid attack. SEM images for the untreated and treated samples, presented in Fig. 8 confirm this effect. It is evident that iron (Fig. 8a) in acidic environment corrodes to a very rough surface (Fig. 8b). With prolonged immersion in inhibitor-containing solution film morphology is changed to smoother and less corroded surface (Fig. 8c).

It is likely that the β-diketone ligand makes complex molecule, i.e., inhibitor molecule adsorption possible by interaction through the part of delocalized O,O′-acetylacetone chelate. Furthermore, conformational flexibility of the *cyclam* plane [37, 38] results in somewhat more stabilizing molecular structure, in which Co(III) and the acetylacetonate form a planar ring and the cyclic amine is folded along an N–Co–N axis that is perpendicular to the Co-*Rac* plane [10].

Molecular modeling and correlation with electrochemical and spectral data

As previously reported, spectral assignments of four Co (III)–*cyclam* β-diketonato complexes are influenced by the presence of different R-groups on the coordinated diketone [8]. Steric and electronic effects of the substituents are seen in the IR and NMR spectra of the complexes. For example, characteristic IR bands are shifted toward higher frequencies. Chemical ^{1}H shifts of the –CH group in the *Rac* ring are regrouped in the high field of parts per million range suggesting strong Co–O bond in the molecule. ^{13}C NMR spectra of the carbonyl diketone group show strong influence of electronic effects of R-supstituents, all in order of the complexes CoT > CoD > CoH with *tmhd* > *dibzac* > *hfac* ligands, respectively [8].

Cyclic voltammetry (CV) data show that the Co(III) complex ion is stable in aqueous solution and the highest stabilization was assigned to CoT [27]. A reverse redox peak in the cathodic region depends on the *Rac* ligand present.

As it can be seen from anticorrosion properties of Co (III)–*cyclam* β-diketonato complexes on iron, the same fundamental approach could be applied to explain slight differences in inhibitor efficiencies. CoT is the best inhibitor and this correlates with the highest stabilization of this complex ion and with a strong influence of the positive inductive effects of the methyl groups (*tert*-butyl

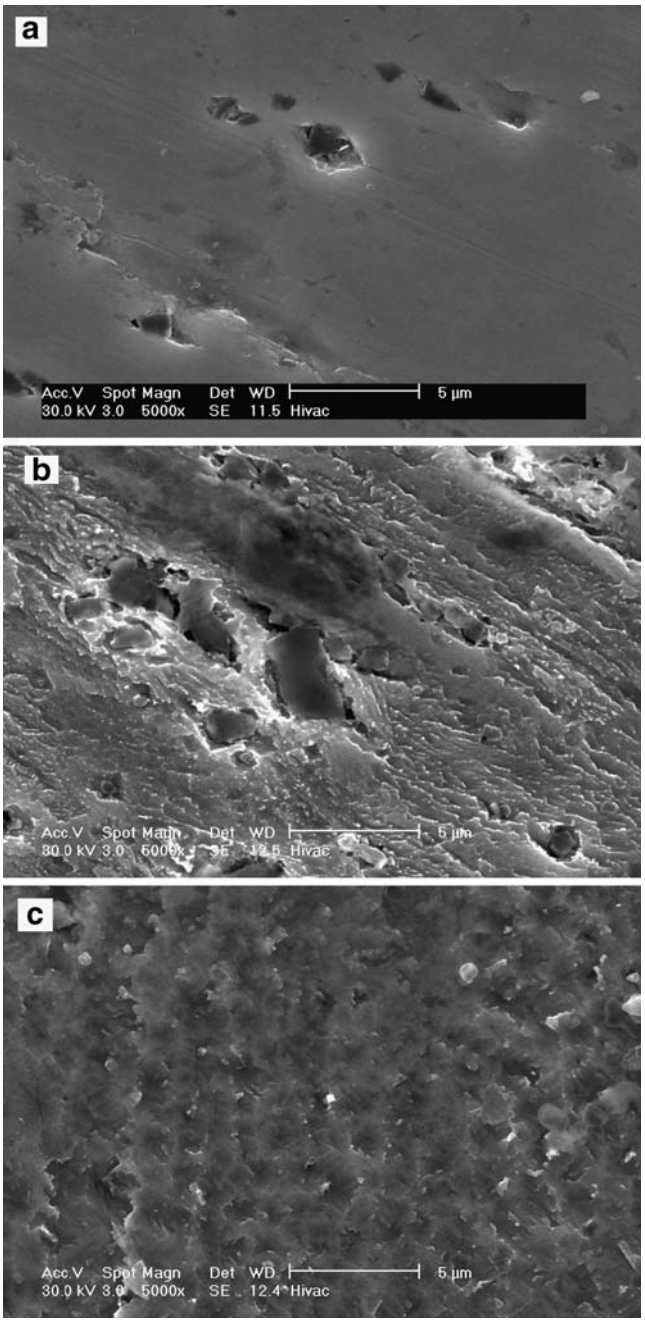

Fig. 8 SEM images of the **a** iron; **b** iron in 0.1 M $HClO_4$ after 1 h immersion; **c** iron in 0.1 M $HClO_4$ after 1 h immersion in the presence of 10^{-3} M CoD

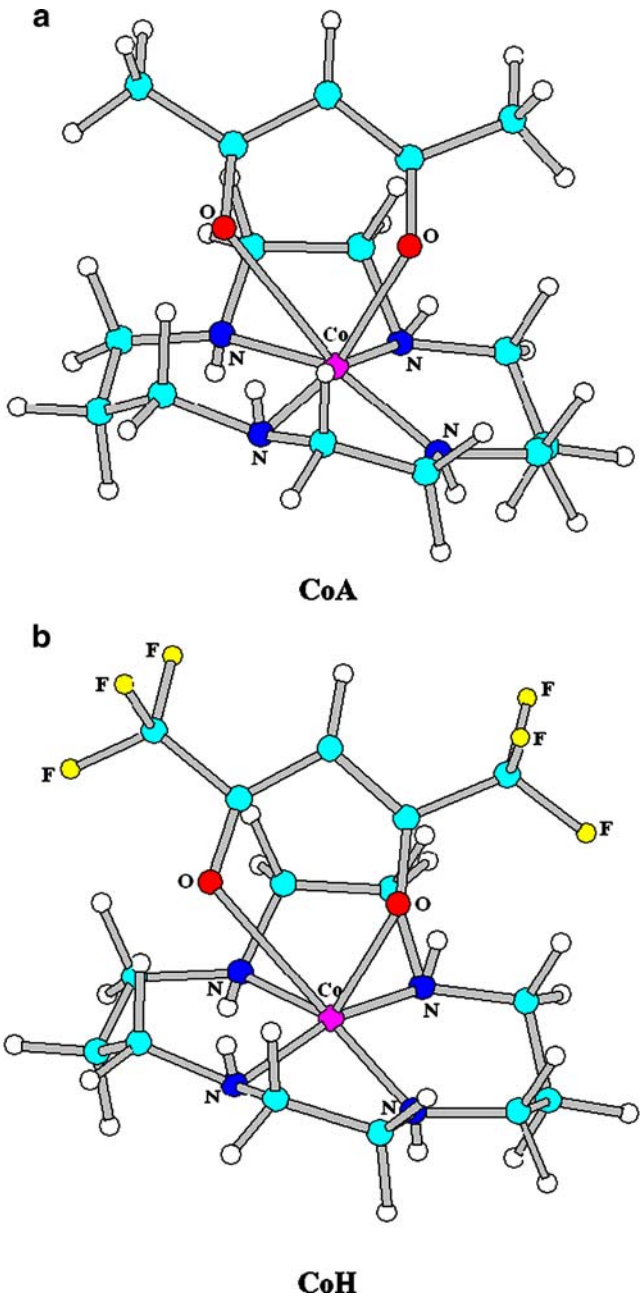

Fig. 9 ZINDO/1 optimization geometry of the complexes **a** [Co(acac)cyclam]$^{2+}$; **b** [Co(hfac)cyclam]$^{2+}$

terminals). This increases electronic density towards the O, O′-chelate ring and consequently shifts characteristic spectral adsorption bands as well as the electrochemical hydrogen evolution to more negative potentials (CV at GC in 0.1 M $NaClO_4$ [27]). On the other side, the trifluoromethyl group is larger and more electronegative than the methyl entity [39]. Its charge density is shifted towards the $–CF_3$ end, while CoT electrons are located along the delocalized part of the β-diketone. Thus, CoH is a poorer inhibitor than CoT. The 1,3-diphenyl group in CoD provides good inhibitor efficiency and high surface coverage because of its additional adsorption center, benzene ring. Therefore, the order of inhibitor efficiency obtained for corrosion on iron in 0.1 M $HClO_4$ can be correlated with some of the previously observed effects within the group of Co(III)–*cyclam* complexes.

Some molecular parameters were calculated within the framework of SCF-MO using the ZINDO/1 method. These calculations may give reliable data for chemical reactivity and point to a relationship with anticorrosion properties of the investigated molecules. The optimized structures for the two of four inhibitors are presented in Fig. 9.

Total charge density of the molecules is displayed mostly on and around the central metal ion and delocalized part of the molecule as well as both of the terminals of the R-diketone. Orientation of such a large complex molecules toward metal surface is important and therefore so is electronic effect of the end-groups. Thus, the presence of an aromatic ring in CoD makes this molecule almost always favorable for effective adsorption, thereby improving its inhibitor properties.

Based on HOMO (highest occupied-) and LUMO (lowest unoccupied-) molecular orbital some global reactivity parameters can be established [40, 41]. For example, for a compound with a large dipole moment a chemical bond with metal surface may be stronger than that for adsorbed water. If so, then inhibitor might displace the water molecules and adsorb via electrostatic bonding. CoT has the highest dipole moment of the group (12.76 D as calculated by ZINDO/1 method) as well as high global softness and electrophilicity, and demonstrates the highest inhibition effect. That criterion is not fully applied for all compounds because the reactivity of the molecule is not defined only with global indexes than in local selectivity in each atom of the molecule when they participate in the corrosion process [41]. Taking in account the complex nature of anticorrosion process further insight into the theoretical approach is necessary for a definitive correlation of structure with inhibition efficiency.

Conclusion

A group of the cobalt(III)–*cyclam* β-diketonato complexes were investigated as corrosion inhibitors for iron in 0.1 M $HClO_4$. The following conclusions were established:

- The corrosion protection in presence of Co(III)–*cyclam* β-diketonato complexes is evident and increase with inhibitor concentration. Inhibitor efficiency increases in the order of CoT > CoD > CoH > CoA.
- Charge transfer resistance, evaluated from EIS spectra, increases with inhibitor concentration. Impedance spectra of CoT and CoH indicate a charge transfer reaction

modeled best by a parallel capacitor and resistor. For CoA and CoD polarization is because of a combination of charge transfer and diffusion processes.
- LPR experiments show strong interaction at the electrode/electrolyte interface that preserves iron surface from the acid attack.
- SEM images give a profile of smoother and less corroded iron surface after treatment in inhibitor-containing solution.
- SCF-MO calculations give reliable data for chemical reactivity and may point to a relationship with anticorrosion properties of the investigated molecules. Also, the order of inhibitor efficiency obtained for corrosion on iron in 0.1 M $HClO_4$ can be correlated with some of the previously observed effects within the group of Co(III)–*cyclam* β-diketonato complexes.

Acknowledgment The authors are pleased to acknowledge the financial support provided by the Robert A. Welch Foundation, Houston, Texas (USA) and Ministry of Science and Ecology of Serbia (project no. 142056).

References

1. Roberge PR (1999) Handbook of corrosion engineering. McGraw-Hill, New York
2. Khaled KF, Babić-Samardžija K, Hackerman N (2006) Corros Sci 48:3014
3. Babić-Samardžija K, Khaled KF, Hackerman N (2005) Appl Surf Sci 240:327
4. Lai TF, Poon CK (1976) Inorg Chem 15:1562
5. Sovilj SP, Vučković G, Babić K, Matsumoto N, Avramov-Ivić M, Jovanović VM (1994) J Coord Chem 31:167
6. Sovilj SP, Vučković G, Babić K, Macura S, Juranić N (1997) J Coord Chem 41:19
7. Sovilj SP, Babić-Samardžija K, Minić DM (1998) J Serb Chem Soc 63:979
8. Sovilj SP, Babić-Samardžija K, Stojšić D (2003) Spectrosc Lett 36:183
9. Sovilj SP, Babić-Samardžija K (1999) Synth React Inorg Met-Org Chem 29:1655
10. Simon E, L'Haridon P, Pichon R, L'Her M (1998) Inorg Chim Acta 282:173
11. Mehrotra RC, Bohra R, Gaur DP (1978) Metal β-diketonates and allied derivatives. Academic Press, New York
12. Kawaguchi S (1986) Coord Chem Rev 70:51
13. Umetani S, Kawase Y, Le THQ, Matsui M (1998) Inorg Chim Acta 267:201
14. Bradley DC, Gaucer D, Mehrotra R (1978) Metal β-diketonates and allied derivatives. Academic Press, London
15. Fackler JP Jr (1966) Prog Inorg Chem 7:361
16. Yang L, Jin W, Lin J (2000) Polyhedron 19:93
17. Seco M (1989) J Chem Educ 66:779
18. Aminabhavi TM, Biradar NS, Divakar MC (1984) Inorg Chim Acta 92:99
19. Cullen WR, Wickenheiser EB (1989) J Organomet Chem 370:141
20. Lewis FD, Miller AM, Salvi GD (1995) Inorg Chem 34:3173
21. Sievers RE, Sadlowski JE (1978) Science 201:217
22. Van Hemert RL, Spendlove LB, Sievers RE (1965) J Electrochem Soc 112:1123
23. Heiner TA, D'Arcangelis ST, Farzad F, Stipkala JM, Meyer GJ (1996) Inorg Chem 35:5319
24. Kimura E (1989) Pure Appl Chem 61:823
25. Jiang J, Kucemak A (2002) Electrochim Acta 47:1967
26. Gouerec P, Biloul A, Contamin O, Scarbeck G, Savy M, Riga J, Weng LT, Bertand P (1997) J Electroanal Chem 422:61
27. Babić-Samardžija K, Sovilj SP, Jovanović VM (2003) J Serb Chem Soc 68:989
28. Pople JA, Beveridge DL, Dobosh PA (1967) J Chem Phys 47:2026
29. Stern M, Geary AL (1957) J Electrochem Soc 104:56
30. McCafferty E, Hackerman N (1972) J Electrochem Soc 119:146
31. Macdonald JR (1987) Impedance spectroscopy. Wiley, New York
32. Scully JR, Silverman DC, Kendig MW (1993) Electrochemical impedance: analysis and interpretation. ASTM International, West Conshohocken, PA
33. Atkins PW (1990) Physical chemistry. Oxford University Press, Oxford
34. Mansfeld F (1990) Electrochim Acta 35:1533
35. Ho C, Raistrick ID, Huggins RA (1980) J Electrochem Soc 127:343
36. Mohamedi M, Takahashi D, Itoh T, Umeda M, Uchida I (2002) J Electrochem Soc 149:A19
37. Costamagna J, Ferraudi G, Matsuhiro B, Campos-Vallette M, Canales J, Villagran M, Vargas J, Aguirre MJ (2000) Coord Chem Rev 196:125
38. Donnelly MA, Zimmer M (1999) Inorg Chem 38:1650
39. Pflaum J, Bracco G, Schreiber F, Colorado R Jr, Shmakova OE, Lee TR, Scoles G, Kahn A (2002) Surf Sci 498:89
40. Elango E, Parthasarathi R, Karthik Narayanan G, Sabeelullah AMd, Sarkar U, Venkatasubramaniyan NS, Subramanian V, Chattaraj PK (2005) J Chem Sci 117:61
41. Gomez B, Likhanova NV, Dominguez Aguilar MA, Olivares O, Hallen JM, Martinez-Magadan JM (2005) J Phys Chem A 109:8950